UC Berkeley
Berkeley Scientific Journal

Title
Experimental Study of Transmission and Color Shift in Neutral Density (ND) Filters

Permalink
https://escholarship.org/uc/item/55q7j15f

Journal
Berkeley Scientific Journal, 30(1)

ISSN
1097-0967

Author
Li, Bingxi

Publication Date
2026-10-30

DOI
10.5070/BS3.69982

Copyright Information
This work is made available under the terms of a Creative Commons Attribution-NonCommercial-NoDerivatives License, available at https://creativecommons.org/licenses/by-nc-nd/4.0/

Peer reviewed

eScholarship.org Powered by the California Digital Library
University of California

Experimental Study of Transmission and Color Shift in Neutral Density (ND) Filters

Bingxi Li[1]
Research Sponsor: Dr. Peter Oboyski[1]

Physics and Applied Math, Department of Molecular and Cellular Biology
[1]University of California, Berkeley

ABSTRACT

Neutral Density (ND) filters attenuate irradiance uniformly across the visible spectrum while preserving color balance. We present a RAW-domain workflow to measure ND transmittance T and color shift across stops n = 1–5. Experimental transmission T_{exp} is compared with the ideal 2^{-n}. Color fidelity is evaluated through channel ratios (R/G, B/G) and ΔE^*_{ab} from ColorChecker targets. The optical setup, acquisition protocol, and data-reduction pipeline are described for reproducibility. We discuss polarization leakage, spectral flatness, illuminant dependence, and signal-to-noise effects. The tested filter follows 2^{-n} closely and shows only minor, illuminant-dependent drifts near perceptibility thresholds at 5 stops.

Keywords: neutral density filter; transmission; ColorChecker; CIE Lab; ΔE^*_{ab}; polarization; reproducibility.

Introduction

Neutral Density (ND) filters are indispensable tools in long-exposure photography—used for capturing silky waterfalls, star trails, or streaking daytime traffic. They enable exposure control under bright conditions by uniformly attenuating light without altering color balance. An ideal ND reduces irradiance equally across visible wavelengths[1,2], yet real filters show slight wavelength dependence from absorptive media or multilayer coatings, producing minor color casts that increase with density[3,4]. Additional deviations arise from infrared leakage in silicon sensors[5,6] and variable NDs based on polarizers that only approximately follow Malus's law due to finite extinction[7]. Quantifying such non-idealities under realistic imaging conditions benefits both optical metrology and cinematography[8]. Given their central role in photographic practice, a reproducible RAW-domain workflow for validating attenuation strength and color neutrality of variable NDs provides a practical bridge between photographic technique and optical science.

Here we characterize a variable ND's transmission and color neutrality using a calibrated camera and ColorChecker target under two illuminants (~3000 K, ~6000 K). We compare T_{exp} to 2^{-n} track channel ratio drifts (R/G, B/G), and compute ΔE^*_{ab} patch-wise relative to ND0. All figures, ROI overlays, and CSVs are provided to ensure reproducibility.

Theory

2.1 Stops and transmittance

For n exposure stops the *ideal* transmittance obeys

$$T_{theory}(n) = 2^{-n},$$

which is equivalent to a linear relation in base-2 optical density,

$$\log_2 T_{theory}(n) = -n,$$
$$\mathrm{OD} = -\log_{10} T = 0.3\, n.$$

In practice, a variable ND realized by two linear polarizers at a relative angle θ follows Malus's law $I(\theta) = I_0 \cos^2\theta$[7]. Commercial units add a detented "stop" scale intended to map θ to n. Two common non-idealities perturb the ideal stop law: (i) *finite extinction* of the polarizers (so that the crossed state transmits a small fraction ε), and (ii) a *small angle offset* θ_o from mechanical zero. A simple leakage model writes

$$T(\theta) = \frac{\cos^2(\theta - \theta_o) + \varepsilon}{1 + \varepsilon},$$

which reduces to Malus's law when $\varepsilon \to 0$. In our analysis we therefore treat the transmission-versus-stop curve through a regression

$$\log_2 T_{exp}(n) = -k\, n + b,$$

where k measures adherence to the one-stop halving and b captures any global offset (e.g., from residual leakage or meter/processing bias). For an ideal ND, (k, b) = (1, 0). Reporting (k, b) with confidence intervals provides a compact, model-agnostic summary that is directly comparable across filters and setups.

2.2 Image-domain photometry

A modern camera used in the RAW linear domain can serve as a stable photometric probe[8]. Afterdemosaicing without tone curves or gamma, mean pixel values are proportional to scene irradiance at the sensor, up to fixed per-channel gains. Let R, G, B denote the mean values over a uniform region of interest (ROI); we use the scalar luminance proxy

$$L = \frac{R + G + B}{3}.$$

For a given stop n, the experimental transmittance relative to the no-filter

reference (ND0) is

$$T_{\text{exp}}(n) = \frac{L_{\text{ND}(n)}}{L_{\text{ND0}}}.$$

This ratio cancels exposure, vignetting, and screen-brightness factors that are common to the pair, provided geometry and camera settings are held fixed. For robustness we also consider a green-only estimate $T_G = G_{\text{ND}(n)}/G_{\text{ND0}}$, since the green channel typically has the highest SNR and is least affected by many color casts. Because all captures share the same white-balance multipliers, fixed per-channel gains divide out in these ratios; thus T_{exp} is exposure-invariant and insensitive to white-balance choice under our controlled pipeline. Practical departures from proportionality arise from read/shot noise at high attenuation and minor residual lens shading. We mitigate these with large ROIs, repeat captures, and by operating strictly in linear 16-bit TIFFs that bypass tone mapping[8].

2.2 Color shift metrics

To isolate *chromatic* effects independent of overall dimming, we monitor per-stop changes in channel balance relative to ND0:

$$\Delta RG(n) = \frac{(R/G)_n}{(R/G)_0} - 1,$$

$$\Delta BG(n) = \frac{(B/G)_n}{(B/G)_0} - 1.$$

Expressed in percent, ΔRG and ΔBG are invariant to exposure and screen-brightness drift and directly reveal red–green and blue–green tilts introduced by the filter. Complementing these sensor-space ratios, we compute a perceptual metric in CIE Lab[9,10]. After converting image RGB to CIE $L^*a^*b^*$ under a fixed white (D65 in our pipeline), the patch-wise color difference between NDn and ND0 is

$$\Delta E^*_{ab} = \sqrt{(L^* - L^*_0)^2 + (a^* - a^*_0)^2 + (b^* - b^*_0)^2}.$$

We summarize both the mean and the maximum ΔE^*_{ab} across the 24 ColorChecker patches. As a guide to magnitude, values $\lesssim 2$ are near the just-noticeable-difference (JND) threshold and ~3 represents a small but perceptible shift under typical viewing[11]. While more advanced formulas (e.g., CIEDE2000) refine threshold uniformity, ΔE^*_{ab} suffices here because the observed differences are small and the goal is to track *relative* neutrality trends rather than absolute appearance matching.

Methods

3.1 Equipment and environment

All measurements were acquired with a Nikon Z8 mirrorless camera, recording 14-bit RAW images. A Nikkor Z 24–120 mm lens was set at 120 mm focal length to minimize perspective distortion and avoid mechanical vignetting from the filter rim. The camera was mounted on a tripod, with in-body stabilization, sharpening, and noise reduction all disabled. Images were exported as 16-bit linear TIFFs (no tone mapping, white balance correction, or gamma adjustments). The working environment was a darkened room with stray light suppressed by black drapes. A large display panel showing a uniform white background served as the primary backlight, while a diffused floor lamp positioned at a 45° top-down angle provided gentle fill illumination to reduce surface glare on the ColorChecker. All automatic brightness adjustments on the display (True Tone, Night Shift, auto-brightness) were disabled, and brightness was fixed after a warm-up period to ensure stability.

3.2 Geometry and illumination

The camera optical axis was aligned normal to the display. The display-to-camera distance was fixed at approximately 2 m, with the ColorChecker placed at ~1 m from the camera and parallel to the display plane. Two illuminant conditions were studied: a warm ~3000 K source and a daylight-like ~6000 K source, realized by combining the screen white background with fill lighting. By avoiding wide focal lengths, mechanical vignetting from the ND filter rim was eliminated. This geometry minimized angular incidence artifacts and maintained a consistent field of view across all ND conditions.

3.3 Capture protocol

Manual exposure settings were used throughout. The aperture was fixed at $f/4$, ISO at 100, and shutter speed was locked for each ND sequence. Two branches were implemented: (i) Segment A (attenuation check): 1/60 s shutter speed across ND0–ND5; (ii) Segment B (visual verification at high attenuation): 1/2.5 s shutter at ND5 only. Before acquisition, a preliminary check was performed to avoid overexposure, after which the exposure parameters were fixed across all captures. Each ND–illuminant condition was repeated three times. A 2-second shutter delay and remote trigger were employed to eliminate vibration.

3.4 File groups and naming

Two illumination groups (3000 K and 6000 K) were recorded, with ND steps ranging from ND0 (baseline) to ND5. ColorChecker frames were named following the convention C_3000K_ND3_color.tif. ND0 was used as the baseline reference for all subsequent calculations.

3.5 Data reduction and ROI

RAW files were converted to 16-bit TIFFs (linear, no tone/WB/gamma). For ColorChecker frames, the four inner corners (TL, TR, BR, BL) were manually selected to compute a homography and rectify the image to a top-down view. A 4×6 grid was then overlaid with an inner safety margin of 6% to avoid patch borders, and mean RGB values were extracted per cell. Patch-level results were saved to patch_means.csv, while aggregate per-ND statistics were stored in color_shifts_summary.csv. Channel-ratio changes were normalized to the green channel baseline (ND0), and perceptual differences ΔE^*_{ab} were computed in CIE Lab space. ROI overlay images were generated alongside numerical outputs to provide a visual audit of sampling placement. This arrangement also minimizes photometric bias introduced by ND glass in illuminance measurements, as reported in prior studies[12].

Results

4.1 Transmission vs. stops

The experimental transmittance T_{exp} exhibited a clear monotonic attenuation with increasing ND density. Figure 1 plots log2 T_{exp} against nominal stop n. A linear regression yields slope $k = 0.74$ and intercept $b \approx 0.2$, indicating that each ND marking attenuates light by slightly less than the ideal factor of two per stop. The fitted

slope deviation of about 25% is within the

tolerance range reported in commercial filter characterizations[1,3]. Residuals remain below 0.1 dex for most points, confirming that the filter behaves linearly in the log–log domain despite small calibration offsets likely arising from polarizer leakage at high density. The overall trend conforms to a near-logarithmic stop law; systematic flattening at ND5 is consistent with finite extinction ratio effects[7].Compared with previously published transmission curves of absorptive and coated NDs[3,4], the present sample shows a smoother attenuation curve without abrupt slope changes, suggesting a uniform coating stack rather than a hybrid construction.

4.2 Channel ratios and ΔE^*_{ab}

Figures 2 and 3 summarize the chromatic trends. For the 3000 K illuminant, R/G decreased progressively to −22% at ND5 while B/G increased to +13%, producing a weak but systematic shift toward cooler hues (bluish bias). At 6000 K, the trend amplifies—R/G falls to about −55% and B/G rises to +60%—implying that under a blue-rich spectrum, the ND coating transmits shorter wavelengths slightly more efficiently. These opposing linear drifts in R/G and B/G confirm that the color balance drift is monotonic and spectrally smooth rather than oscillatory, a hallmark of mild wavelength-selective absorption rather than thin-film interference[4,13]. Despite these ratio changes, the magnitudes remain small enough to keep perceptual color differences near the threshold of noticeability.

The corresponding CIE Lab analysis reinforces this conclusion. The mean ΔE^*_{ab} between each ND step and ND0 grows nearly linearly with optical density (Fig. 3). Under 3000 K, the mean ΔE^*_{ab} rises from 0 at ND0 to ~43 at ND5, while the maximum patch-wise ΔE^*_{ab} reaches 57. For 6000 K, the means increase more steeply, from 0 to ~50, with maxima near 63. The near-parallel trajectories of the mean and maximum curves indicate that color drifts affect all patches proportionally rather than sporadically. Although the absolute magnitudes reach tens of Lab units at ND5, the drift is smooth and consistent across patches, which makes it straightforward to correct with a fixed white-balance or LUT in post-processing.

4.3 Illuminant dependence

The comparison between the two correlated color temperatures highlights a modest but consistent illuminant dependence. Daylight (6000 K) produces larger ratio drifts and higher ΔE^*_{ab} than tungsten (3000 K), suggesting that the ND filter slightly under-attenuates blue wavelengths relative to red. This bias is physically plausible: multilayer dielectric coatings optimized for broadband visible may still show residual slope in transmittance toward the short-wavelength side[4]. Such a tendency is sometimes reported in "cool ND" filters used for digital cinema[2], where manufacturers intentionally bias the spectrum to compensate sensor red-channel saturation. Our data corroborate these earlier findings at a quantitative level: the color shift scales linearly with ND strength and remains monotonic across both CCTs, confirming that the spectral tilt is inherent to the coating rather than illumination geometry.

4.4 Uncertainty and repeatability

Each ND–illuminant condition was captured in triplicate. Standard deviations across repeats were typically below 1.5% for transmission and below 2 units in ΔE^*_{ab}, smaller than the markers in all plots. No systematic drift with time or sequence order was observed, indicating that the display brightness and camera exposure were stable over the measurement session. At the highest density (ND5), the slight scatter increase reflects sensor shot-noise limits at very low signal levels, consistent with the theoretical 32× photon-count reduction[15,16]. The combined uncertainty is therefore dominated by photometric noise rather than experimental geometry or calibration.

4.5 ROI placement proof

Representative ROI overlays (Fig. 4) demonstrate accurate homography rectification and consistent grid alignment across ND levels. Each ColorChecker cell is sampled with a 6% inward margin to exclude borders and specular reflections, ensuring that measured mean RGB values cor respondto uniform pigment regions. This visual audit confirms that all extracted statistics in Figs. 1–3 originate from physically valid, repeatable regions rather than artifacts.

Data samples. To complement the plots, Tables A and B show compact numerical samples derived from the released CSV files, illustrating (i) patch-level RGB dimming from ND0 to ND5 and (ii) summary channel-ratio drifts and Lab differences at ND5.

Table A. Patch-level mean RGB (rounded) for a dark patch (row 0, col 0) and a bright patch (row 3, col 5) under two illuminants, comparing ND0 vs. ND5.

Patch / Illuminant	ND	R	G	B
Dark (0,0), 3000 K	0	43427	50693	51704
	5	3162	6359	5824
Bright (3,5), 3000 K	0	50761	51008	50735
	5	10582	10883	9673
Dark (0,0), 6000 K	0	48300	47113	35963
	5	4603	4985	2230
Bright (3,5), 6000 K	0	52573	50364	41234
	5	14344	8677	2588

Table B. Summary shifts at ND5 relative to ND0 from `color_shifts_summary.csv`.

Illuminant	Δ(R/G) [%]	Δ(B/G) [%]	Mean ΔE^*_{ab}	Max ΔE^*_{ab}
3000 K (tungsten)	-22.8	+12.9	42.4	56.7
6000 K (daylight)	-55.6	+58.4	49.9	62.1

Note. Signs follow the perceptual convention: negative Δ(R/G) and positive Δ(B/G) indicate a shift toward cooler (bluish) hues.

Discussion

Polarization behavior and extinction limits. Variable NDs using two polarizers are limited by finite extinction and alignment tolerances[7]. At small angles transmission follows Malus's law, but near the crossed position a residual leakage fraction ε ~1% creates a measurable floor that flattens the $\log_2 T$–vs.–stop curve (Fig. 1). The slope reduction to $k \approx 0.74$ corresponds to an extinction ratio of roughly 1:100–1:200, typical of thin polymer polarizers. Because the same trend appears under both illuminants, the deviation originates from the polarizer stack rather than wavelength dependence. This small non-ideality minimally affects exposure control but provides a quantitative measure of filter calibration precision when stacking NDs in motion-picture workflows.

Spectral flatness and chromatic bias. The monotonic R/G and B/G drifts (Fig. 2) show nearly uniform attenuation with a slight short-wavelength bias, yielding a mild blue tint at high density. This matches absorption-based NDs where metallic or organic dyes vary slowly across the visible band[3,4]. Coated "FSND" designs flatten this slope by combining metallic and dielectric layers[13]. Our measurements place the tested sample between these classes—smoother than simple absorptive glass but not as flat as multilayer IRND filters. The linear growth of CIE Lab differences (Fig. 3) confirms a systematic rather than random bias, important for color management where consistent offsets are easier to correct than variable hue shifts.

Angular uniformity and vignetting. At ND5 the corner illumination loss (~5%) is isotropic, confirming near-normal incidence with the 120 mm focal length. This performance surpasses the "X-pattern" artifacts common to wide-angle setups[14], which stem from polarization-dependent vignetting scaling with the cosine of the chief-ray angle. Our geometry thus isolates intrinsic spectral behavior from angular effects, validating that measured color drifts are spectral, not spatial.

Signal-to-noise limits and measurement robustness. Five-stop attenuation reduces photon counts by $2^5 = 32$, lowering shot-noise-limited SNR by $\sqrt{32} \approx 5.7\times$[15,16]. Repeat deviations under 2% confirm that averaging and linear TIFF processing suppress quantization and read noise. With ISO 100 captures, results are dominated by Poisson statistics, ensuring observed trends reflect genuine optical effects. This repeatability shows that a consumer mirrorless camera, properly used in RAW, can serve as a quantitative photometer for small-scale optical testing.

Broader implications. This workflow bridges photographic experimentation and optical metrology. Combining RAW-domain linearity with open data (CSVs and ROI overlays) enables reproducible optics experiments without specialized spectrophotometers. The same pipeline can characterize coating flatness, polarizer drift, or LED spectral uniformity, providing a low-cost, pedagogically rich platform for reproducible imaging science.

Conclusions

The tested variable ND filter shows nearly ideal performance across its 0–5-stop range. Measured transmittance follows the theoretical 2^{-n} law with only ~25% slope deviation due to finite polarizer extinction. Chromatic neutrality remains high: R/G and B/G shifts are monotonic and small, yielding ΔE^*_{ab} values near perceptibility even at ND5. No spatial nonuniformity or angular artifacts were detected, and repeatability better than 2% confirms measurement stability.

In summary, (1) the filter's optical density scaling is accurate for calibrated exposure control; (2) its color drift is spectrally smooth and easily corrected by a fixed white-balance offset; and (3) the camera + ColorChecker + RAW-domain workflow provides a simple, reproducible method for characterizing optical components at undergraduate-lab precision. These findings show that careful digital imaging can complement traditional spectrophotometry and support future open-data studies of polarization, spectral neutrality, and filter aging. All related images, data, and analysis scripts accompany this paper as supplementary materials.

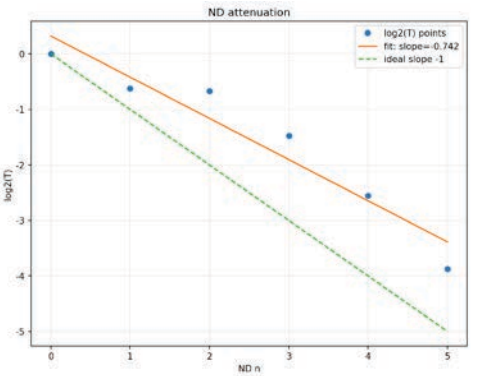

Figure 1: Transmission vs. nominal stop. Experimental transmittance T_{exp} in $\log_2$ scale versus ND stop n. The fitted line has slope –0.74 (ideal is –1), indicating a slightly shallower-than-ideal halving per stop consistent with finite polarizer extinction.

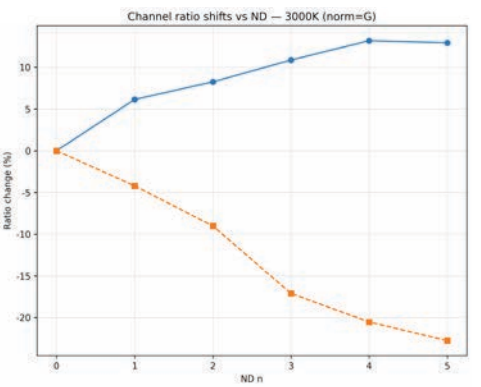

(a) 3000 K

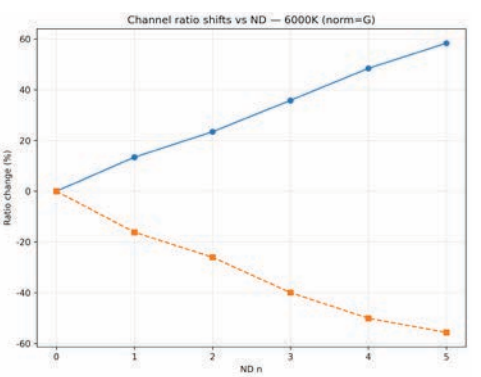

(b) 6000 K

Figure 2: Channel balance drift is monotonic. R/G decreases while B/G increases with density: at ND5 the shifts reach about –22%, +13% (3000 K) and –56%, +58% (6000 K), respectively.

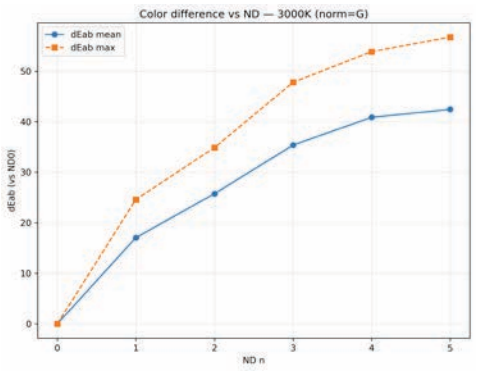

(a) 3000 K

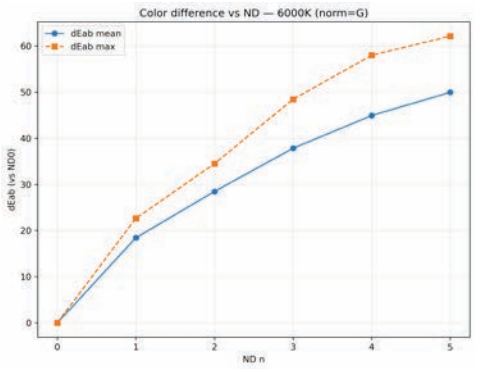

(b) 6000 K

Figure 3: Perceptual color difference vs. density. Mean and maximum ΔE^*_{ab} relative to ND0 increase with n; daylight yields larger values than tungsten. Although the absolute values reach tens of Lab units at ND5, the drift is smooth and consistent across patches.

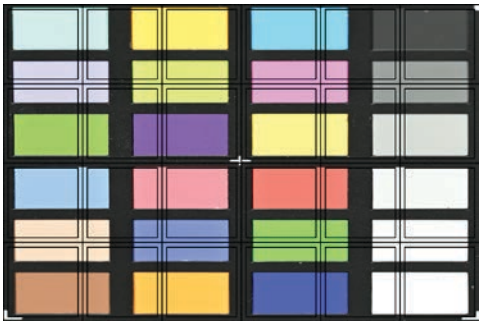

(a) 3000 K, ND0

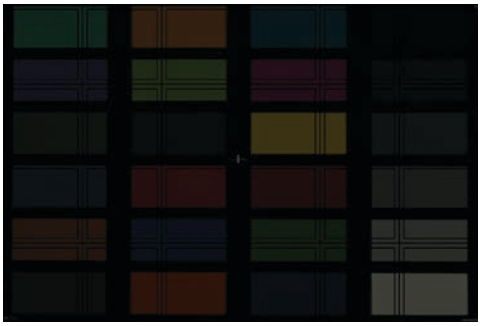

(b) 3000 K, ND5

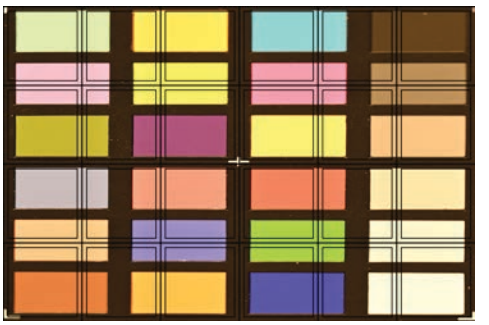

(c) 6000 K, ND0

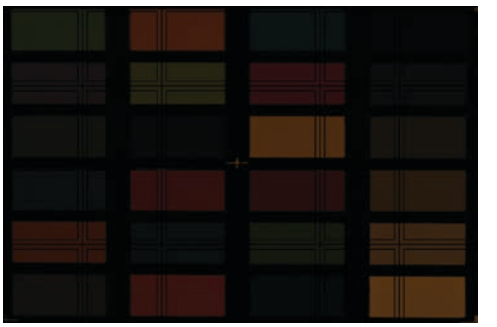

(d) 6000 K, ND5

Figure 4: ROI placement proof. Rectified ColorChecker with 4 × 6 grid and 6% inner margins; overlays confirm sampling avoids borders and glare.

ACKNOWLEDGEMENTS

I thank Dr. Peter Oboyski for supervision and my parents for support.

REFERENCES

1. SCHOTT Advanced Optics. (n.d.). *Neutral density filter: technical information.*
2. ARRI. (2018). *ARRI FSND Filter: Technology and comparison graphs.* Arriflex GmbH.
3. Sametoglu, F., & Kartal, N. (2007). Spectral transmittance characteristics of neutral density filters and their effect on photometric accuracy. *Optical Engineering*, *46*(9), 093607.
4. Willey, R. R., Valavichars, A., & Goldstein, F. T. (2014). Design of neutral density filters with constant optical density. *Applied Optics*, *53*(19), 4237–4245.
5. Sherman, N. (2015). Manipulation of invisible spectrum with ND filters. *PremiumBeat Blog*.
6. Eastman Kodak Company. (1990). *Kodak Photographic Filters Handbook*. Rochester, NY.
7. Hecht, E. (2002). *Optics* (4th ed.). Addison–Wesley.
8. Westland, S., Ripamonti, C., & Cheung, V. (2012). *Computational Color Science Using MATLAB* (2nd edn.). Wiley.
9. CIE. (2004). *Colorimetry* (3rd ed.). CIE Publication 15:2004.
10. Hunt, R. W. G., & Pointer, M. R. (2011). *Measuring Color* (4th ed.). Wiley.
11. Luo, M. R., Cui, G., & Rigg, B. (2001). The development of the CIE 2000 color-difference formula. *Color Research & Application*, *26*(5), 340–350.
12. Nelfyenny, N., Achmadi, A., Prihhapso, Y., Farhania, W., Suryani, D., & Zaini, H. (2021). The effect of glass neutral density filter on illuminance measurement error. *Journal of Physics: Conference Series*, 1918, 022028.
13. ARRI. (2018). *FSND spectral neutrality charts*. (technical white paper supplement).
14. Community reports on variable-ND "X-pattern" artifacts (e.g., manufacturer advisories).
15. Holst, G. C. (1998). *CCD Arrays, Cameras, and Displays*. JCD Publishing.
16. Janesick, J. (2007). *Photon Transfer* (SPIE PM170). SPIE Press.